I&EC research
Industrial & Engineering Chemistry Research

Article

pubs.acs.org/IECR

Deoxygenation of *m*-Cresol: Deactivation and Regeneration of Pt/γ-Al_2O_3 Catalysts

M. S. Zanuttini, M. A. Peralta, and C. A. Querini*

Instituto de Investigaciones en Catálisis y Petroquímica (INCAPE), FIQ, UNL, CONICET, Santiago del Estero 2654, Santa Fe, S3000AOJ, Argentina

ABSTRACT: Pt/Al_2O_3 catalysts were used to deoxygenate *m*-cresol, which was used as a bio-oil model compound. The catalysts were characterized by XRD, TEM, XPS, hydrogen chemisorption, and BET surface analyses. The coke deposits on spent catalysts were analyzed by TPO. In this work, the catalysts deactivation and regeneration were addressed. Deactivation was caused by carbonaceous deposits formed mainly by cresol condensation products, in a parallel-type coke formation mechanism. The amount of carbon formed on the catalyst strongly depends on the metal/acid functions ratio. The gas phase reaction was carried out in a fixed bed reactor in the presence of H_2 at 300 °C and atmospheric pressure. The regeneration by coke removal using hydrogen or air was addressed. It was found that treatments in air at mild temperature led to the recovery of the catalytic activity, while the effectiveness of the treatment with H_2 strongly depends on the temperature, not being possible to recover the activity at 400 and 500 °C, while at 450 °C the catalyst was regenerated. This is because at the higher temperature, the coke left on the support had higher toxicity. The influence of platinum loading on activity and selectivity was also studied, and it was concluded that the selectivity to the desired deoxygenated product can be regulated by changing the metal content on the catalyst. The metal/acid sites ratio plays a key role in the coke deposition rate.

1. INTRODUCTION

The liquid bio-oil obtained by biomass fast pyrolysis is a potential fuel that after upgrading can be mixed with nonrenewable fuels. These treatments are necessary, since the high oxygen contents of bio-oil impart negative properties to it because of its high viscosity, low heating value, corrosiveness, and instability.[1−3] Moreover, the high reactivity complicates the use of bio-oil as a fuel and its long-term storage. Catalytic deoxygenation of bio-oil is one of the possible treatments for bio-oil upgrading.[4−14]

The Pt/Al_2O_3 catalyst was previously studied in the hydrodeoxygenation of *m*-cresol, which was selected as a model compound of the bio-oil.[15] The main hydrodeoxygenation products were toluene, benzene, and methylcyclohexane, and the selectivity to these products depended on the reaction conditions. It was shown that the yield of the desired product can be regulated by changing the metal loading, the H_2/cresol ratio, and the reaction temperature. The toluene hydrogenation to methylcyclohexane was favored at low temperature, while the toluene yield has a maximum at an intermediate temperature level (around 300 °C), since at high temperatures toluene was transformed into benzene by demethylation. The amount of coke deposited during *m*-cresol deoxygenation on the Pt/γ-Al_2O_3 is rather low, about 1 wt %. The initial activity was high, but deactivation was observed.

It was shown that catalyst deactivation was mainly due to cresol condensation products, since the coke percentage on spent catalysts decreased as a function of the contact time (W/F), suggesting that the main deactivation mechanism was a parallel coking path,[15] being the coke formed mainly from the reactant. The deactivation and regeneration of metallic catalysts used in phenolics compounds deoxygenation were scarcely studied. Ausavasukhi et al.[16] studied the deoxygenation of *m*-cresol over Ga-modified H-Beta (Ga/HBEA) zeolites and proposed that a major fraction of the feed gets strongly adsorbed inside the zeolite, forming a "surface pool" of oxygenated species. These authors also observed that the hydrogenolysis of trapped products as well as of the larger molecular aggregates that have started to condense was greatly accelerated in the presence of Ga and H_2 in the gas phase.

Foster et al.[17] studied the deoxygenation of *m*-cresol with Pt/Al_2O_3 and Pt/SiO_2 at 0.5 atm and observed that the catalysts deactivated. However, the activity and selectivity toward toluene were recovered after regeneration of Pt/Al_2O_3 in H_2 at 450 °C and 0.5 atm. In contrast to the alumina-supported sample, postreaction treatment in H_2 did not restore activity for the Pt/SiO_2 catalyst. The treatment in H_2 caused a decrease in the conversion of *m*-cresol and its selectivity toward toluene. According to Foster et al.[17] the Pt metal−support interaction is much weaker on the SiO_2 support than on Al_2O_3, and consequently Pt/SiO_2 is more susceptible to particle sintering. The presence of hydrogen has been shown to facilitate the diffusion of Pt, and combined with the weaker interaction between Pt and SiO_2, a faster sintering of the Pt particles occurred. The study of Foster et al.[17] is the only publication that partially addressed the regeneration of hydrodeoxygenation (HDO) catalysts but without including a detailed study of the coke deposits.

H_2 not only reacts in hydrodeoxygenation but also inhibits the formation of undesirable heavy products. Thus, the hydrodeoxygenation of methyloctanoate over Pt/Al_2O_3[18] yields mainly C7 alkanes and alkenes by decarbonylation or

Received: January 22, 2015
Revised: April 17, 2015
Accepted: April 20, 2015

DOI: 10.1021/acs.iecr.5b00305
Ind. Eng. Chem. Res. XXXX, XXX, XXX−XXX

decarboxylation of the ester, acid, or other oxygenate. When deoxygenation is carried out under inert gases, heavy products such as diheptylketone, *n*-pentadecane, and octyloctanoate are formed.

In the present work, the catalyst deactivation and regeneration are addressed, as well as the influence of metal loading on product distribution and deactivation. A detailed investigation of the relationship between types of coke and activity/selectivity of HDO bifunctional catalysts is presented. The objective is to determine the effect of different operating variables on the amount of coked formed on Pt/γ-Al_2O_3 catalysts and the nature of the coke deposits and to study the effect of the regeneration strategy on the activity recovery. The use of hydrogen to regenerate the catalyst is also investigated, with the objective of developing a simple process in which the regeneration is carried out without the need of switching gases as is the case when air is used.

The effect of the metal loading on the deactivation and coke formation is also addressed.

2. EXPERIMENTAL SECTION

2.1. Preparation of Catalysts. The catalysts were prepared by wet impregnation of platinum precursor on γ-Al_2O_3 support (CK-300 from Cyanamid Ketjen). Tetraamineplatinum(II) nitrate (metal content 50%) was supplied by Alfa Aesar. An aqueous solution of 1% of $Pt(NH_3)_4(NO_3)_2$ was used to prepare the catalyst. A suspension of γ-Al_2O_3 in the metal precursor solution was stirred on a hot plate at 110 °C until complete evaporation. The impregnated catalyst was dried in an oven at 110 °C for 12 h. The dried sample was calcined in air flow (Air Liquide >99.99%) in an electric furnace at 350 °C for 2 h. The platinum content was varied between 0.05 and 1.7 wt %.

2.2. Characterization of Catalysts. The specific surface area and porosity were determined from nitrogen adsorption−desorption isotherms, which were recorded at liquid-nitrogen temperature and relative pressure (P/P_o) interval between 6×10^{-7} and 0.998 on a Quantachrome equipment. Samples were evacuated prior to measurements at 523 K for 3 h under a vacuum of 1×10^{-5} Pa. The BET model was used in the relative pressure range 0.01−0.10 to calculate the total surface area.

Catalyst crystalline structures were characterized by X-ray diffraction (XRD). The X-ray diffractograms were obtained with a Shimadzu XD-D1 instrument with monochromator using Cu Kα radiation at a scanning rate of 4° min^{-1}, from 2θ = 5° to 2θ = 100°.

Reducibility of metallic catalysts was studied by temperature-programmed reduction (TPR) analyses. These experiments were carried out in an OKHURA TP-2002S system, equipped with a thermal conductivity detector (TCD), heating the sample at 10 °C·min^{-1} in 5% H_2/Ar (30 mL·min^{-1}). The temperature was increased from 20 to 900 °C.

Particle size distributions were determined by transmission electron microscopy (TEM). The reduced samples were placed in distilled water. One drop of this suspension was then placed on holey carbon supported on a copper grid. The micrograph images of the samples were acquired with a JEOL 100 CX model microscope at 100 kV, and a magnification of 450 000×. The metallic dispersions were calculated using the following equations:[19,20]

$$d_{Pt} = \frac{0.821}{D_{Pt}} \quad (1)$$

where D_{Pt} is the metallic dispersion and d_{Pt} is the particle size (D_{VA}) in nm. D_{VA} is a volume−area average size defined as follows:

$$D_{VA} = \frac{\sum n_i d_i^3}{\sum n_i d_i^2} \quad (2)$$

The amount of carbonaceous materials deposited on the spent catalysts was determined by temperature-programmed oxidation (TPO), using a stream of 5 v/v% O_2 in N_2 and a heating rate of 12 °C·min^{-1}. The oxidation products were detected with a flame ionization detector (FID) after methanation. Further details can be found elsewhere.[21]

The hydrogen chemisorption measurements were made in volumetric equipment at room temperature. The sample used in the experiments was previously outgassed under vacuum (10^{-4} Torr). The hydrogen adsorption isotherms were performed at room temperature between 25 and 100 Torr. The isotherms were linear in the range of used pressures, and the hydrogen chemisorption capacity was calculated by extrapolation of the isotherms to zero pressure,[22] assuming a H/Pt = 1 adsorption stoichiometry.

The chemical state of Pt was determined by X-ray photoelectron spectroscopy (XPS). The XPS analyses were performed in a multitechnique system (SPECS) equipped with a dual Mg/Al X-ray source and a hemispherical PHOIBOS 150 analyzer operating in the fixed analyzer transmission (FAT) mode. The samples were mounted on a sample rod, placed in the pretreatment chamber of the spectrometer, submitted to a reduction in H_2/Ar during 10 min, and then evacuated at room temperature. The spectra were obtained with pass energy of 30 eV. The spectra were processed using the software Casa XPS (Casa Software Ltd., U.K.). The intensities were estimated by calculating the integral of each peak after subtracting a Shirley-type background and fitting the experimental curve to a combination of Lorentzian and Gaussian lines. Binding energy values were referenced to the C1 peak (284.6 eV). For the quantification of the elements, sensitivity factors provided by the manufacturers were used.

2.3. Catalytic Activity. The catalytic activity was measured at atmospheric pressure in a continuous-flow fixed-bed reactor, made with a quartz tube of 5 mm internal diameter. The catalyst was ground and sieved and the 40−80 mesh fraction used for the catalytic tests. The catalyst bed was supported with quartz wool. Above the catalytic bed, quartz beads were loaded in order to improve the heat transfer. The catalyst was pretreated under flow of H_2 (Air Liquide, >99.9990%) (30 mL·min^{-1}) by heating at 10 °C min^{-1} from room temperature to 500 °C and maintained at this temperature for 1 h. The catalyst was then cooled to the reaction temperature (300 °C). The carrier was bubbled in liquid cresol (Merck, >99%) maintained at a preselected temperature in the range 40−90 °C, in order to saturate the gas. The carrier flow rate was 5−50 mL·min^{-1}. Under these conditions the cresol partial pressure in the gas stream fed to the reactor was between 0.51 and 107.2 Torr, and the contact time (W/F) was between 2.5 and 80 g_{cat}·h·$(g_{cresol})^{-1}$. After each run, the catalyst bed was purged with H_2 at the reaction temperature during 30 min. The gas flow rates were controlled with mass flow controllers (Aalborg Instruments and Controls, Inc.). The reactor outlet stream was

DOI: 10.1021/acs.iecr.5b00305
Ind. Eng. Chem. Res. XXXX, XXX, XXX−XXX

analyzed in a GC (SRI 8610) connected online and equipped with a ZB-5 capillary column (15 m) and FID detector. A split ratio of 100 was used. Standard samples were used in order to identify the reaction products. In addition, a GC−MS (Varian Saturn 2000) equipped with a HP-5 capillary column was used to identify the reaction products collected in a condenser cooled at 0 °C. The noncondensed gases were analyzed by GC using a Petrocol (Supelco) capillary column (100 m). The products were identified by GC analysis using pure chromatographic standards and also by GC−MS.

To determine if there is conversion due to thermal decomposition, an experiment without catalyst was carried out at 500 °C. Pure alumina was also tested at 300 °C, W/F = 11.3 $g_{cat}\cdot h\cdot(g_{cresol})^{-1}$, and H_2/cresol molar ratio of 510.

In order to evaluate catalytic activities at similar conversions, the W/F was varied using different values for each catalyst, changing from 79.9 $g_{cat}\cdot h\cdot(g_{cresol})^{-1}$ for the Pt(0.05)/γ-Al_2O_3 to 2.5 $g_{cat}\cdot h\cdot(g_{cresol})^{-1}$ for the Pt(1.7)/γ-Al_2O_3. The effect of contact time on coke deposition was studied with the Pt(1.7)/γ-Al_2O_3 catalyst varying the W/F, between 37 and 0.1 $g_{cat}\cdot h\cdot(g_{cresol})^{-1}$. The different contact times (W/F) were obtained by changing the catalyst mass loaded in the reactor and the hydrogen flow rate, maintaining constant the saturator temperature. The H_2/m-cresol molar ratios used were 197 and 510. The time on stream was 6.5 h in both cases.

With the objective of evaluating the effect of the H_2/cresol molar ratio, its value was varied by mixing H_2 and N_2 and fixing the total flow rate (30 mL min^{-1}) and the W/F (6.4 and 0.1 $g_{cat}\cdot h\cdot(g_{cresol})^{-1}$). For regeneration experiments the value of W/F used was 0.08 $g_{cat}\cdot h\cdot(g_{cresol})^{-1}$ and the H_2/m-cresol molar ratio was 64 and 111. A reaction test was performed during 140 min, and online samples were analyzed with GC. Afterward, a treatment was performed. For the case where air is used, a subsequent in situ activation of the catalyst in H_2 was necessary. After each treatment, reaction test was performed at the same conditions of the first 140 min.

The absence of internal and external mass transfer limitations was verified using different catalyst particle sizes (40−80 mesh and a fraction with particles smaller than 200 mesh) at W/F = 0.4 $g_{cat}\cdot h\cdot(g_{cresol})^{-1}$) and H_2 flow rates (5.5 and 50 cm^3/min) at two different W/F (0.08 and 37 $g_{cat}\cdot h\cdot(g_{cresol})^{-1}$). Under these conditions, which are the extreme values used in this study for each variable, similar conversions and product distributions were obtained. No heat-transfer limitations are expected, since the heats of reaction are relatively small.

Two sets of experiments corresponding to W/F = 0.48 $g_{cat}\cdot h\cdot(g_{cresol})^{-1}$ and W/F = 38 $g_{cat}\cdot h\cdot(g_{cresol})^{-1}$ were repeated 5 times. A good reproducibility was achieved. Relative standard deviation of product yields was 8%.

Carbon balances after the catalytic tests were calculated. The number of moles of C fed was considered as the amount of reactant fed during the reaction time ($moles_1$) multiplied by the number of C per molecule of reactant (ν_1), as indicated in eq 3. The number of moles of C at the reactor outlet was calculated as the sum of the moles of C for all the products and the nonconverted reagent obtained by chromatographic analysis (eq 4). Since the "light products" were not analyzed in detailed in all samples and represent a lump of products, the carbon balance was carried out in two extreme situations. In one case, it was supposed that the light products were just methane (one C molecule) and in the other case assuming six C molecules. The average values of product yields and reactant conversion during the reaction were considered for the calculation of the moles at the reactor outlet.

Furthermore, the carbon deposited on the catalyst (eq 5) was taken into account. It was calculated using the mass of catalyst used in the experiment (m_{Cat}) and the coke content determined by TPO analysis.

Total moles of C fed to the reactor during the reaction time was

$$n^{\circ}C_{Feed} = moles_1 \times \nu_1 \tag{3}$$

Total moles of C at the reactor outlet during the reaction time was

$$n^{\circ}C_{Outlet} = \sum_{i=1}^{n} (moles_i \times \nu_i) \tag{4}$$

where i = 1 is the reactant, i = 2, 3, ..., n are products, and ν_i is the number of C atoms in molecule i.

Total moles of C deposited on the catalyst during the reaction time was

$$n^{\circ}C_{Cat} = \frac{[\%C(TPO)]m_{Cat}}{[12\ (g/mol)]100} \tag{5}$$

where %C(TPO) is the percentage obtained by TPO analysis and m_{Cat} is the catalyst mass used in the experiment.

Finally the recovery percentage was calculated using (eq 6),

$$\%\ recovery = \frac{(n^{\circ}C_{Outlet} + n^{\circ}C_{Cat})}{n^{\circ}C_{Feed}} \times 100 \tag{6}$$

2.4. Regeneration. The regeneration experiments were carried out using a W/F of 0.08 $g_{cat}\cdot h\cdot(g_{cresol})^{-1}$ and H_2/m-cresol molar ratios of 64 and 111. The reaction test was performed for 140 min, and samples were analyzed online with a GC. Then the catalyst was regenerated for different times, using either air ((Air Liquide >99.99%) at 350 °C or hydrogen (Air Liquide >99.999%) at 500 °C. In the case in which air was used, prior to the regeneration the reactor was purged with nitrogen, and after the regeneration a subsequent in situ activation of the catalyst in H_2 was necessary. After this reduction, a new reaction cycle was carried out, as indicated above.

3. RESULTS AND DISCUSSION

3.1. Characterization of Catalysts. The characterization results of the catalysts used in this study were recently reported.[15] A summary of the most relevant information is presented in this section to help in the discussion of the deactivation and regeneration studies.

The X-ray diffractograms presented the typical signals of the γ-Al_2O_3 at 2θ = 45.901, 67.093, 37.635, 39.524, and 19.466 (JCPDS-ICDD 10-425). No signals corresponding to Pt crystals were detected in any of the catalysts studied, which indicates that the metal particles were small.

The histograms of the distribution of particle size obtained for Pt(1.7)/γ-Al_2O_3 and Pt(0.05)/γ-Al_2O_3 showed that the Pt was highly dispersed in all samples, with particle diameter on the order of 14 Å. The dispersion corresponding to this value was 60%, as calculated with eqs 1 and 2. Nevertheless, even though the mean particle size was not very different between the Pt(1.7) and Pt(0.05) catalysts, there was an evident difference in the amount of smaller particles. The catalyst with 0.05% Pt had an important fraction of particles with diameter

DOI: 10.1021/acs.iecr.5b00305
Ind. Eng. Chem. Res. XXXX, XXX, XXX−XXX

below 1.2 nm. However, this difference in particle sizes with the loading of Pt was not significant in order to affect the product selectivity.

The metallic dispersion obtained by hydrogen chemisorption with Pt(1.7)/γ-Al_2O_3 catalyst was 55%, in agreement with the value obtained by microscopy.

The TPR profile of Pt(1.7)/γ-Al_2O_3 displayed two peaks, one at 240 °C and the second at 414 °C, which can be assigned to the bulk phase of the PtO_x and to highly dispersed particles with strong interaction with the support, as previously reported.[23−25]

The surface area, pore volume, and pore diameter were similar for the catalysts with different Pt loadings, approximately 195 $m^2 \cdot g^{-1}$, 0.49 $mL \cdot g^{-1}$, and 88 Å, respectively. The γ-Al_2O_3 catalytic surface area was 200 $m^2 \cdot g^{-1}$. The preparation procedure had little effect on the BET area, pore volume, and pore diameter, and consequently, it can be expected that the activity results were not influenced by these negligible changes.

The XPS analyses were obtained with the Pt(1.7)/γ-Al_2O_3 catalyst after reduction at 500 °C. Although the most intense photoemission lines of platinum are those arising from the 4f levels, this energy region is overlapped by the Al 2p line of γ-Al_2O_3. Therefore, the Pt 4d line was used.[15] This one is weaker, but it is not overlapped by spectral lines of other components. The decomposition of the spectra into individual components revealed the presence of two platinum states: the reduced state (Pt^0) with a binding energy (Eb) of 314.1 eV and the oxidized state with a Eb of 317 eV, and the percentages of the different states of platinum were 59% and 41% for Pt^0 and PtO_x, respectively. As stated by Serrano-Ruiz et al., even after reduction at 500 °C, Pt seems to maintain some δ^+ character, which indicates the presence of a metal−support interaction.[26] However, it has to be noted that the fraction of the platinum oxidized in the XPS spectrum may not correspond to the real concentration of oxide. Ivanova et al.[27] showed that according to the HRTEM data, platinum oxide in a sample of Pt/Al_2O_3 existed as large particles. Thus, the signal intensity is, in addition to other factors, related to the dispersion. A high intensity in the XPS spectrum indicates higher dispersion. This means that in the case of having a low concentration of small particles, it may display a more intense signal than with larger particles.[27] It is also possible that the δ^+ character is due to the migration of oxygen from the bulk to the surface of the particles.

The acid site density on the Pt(1.7)/γ-Al_2O_3 determined by pyridine temperature-programmed desorption was 0.296 μmol $Py \cdot m^{-2}$.[28] The effect of the acid sites density and strength was analyzed by Zanuttini et al.,[28] working with eight different catalysts. It was concluded that a low concentration of acid sites, such as that displayed by the Pt(1.7)/γ-Al_2O_3 catalyst (0.296 μmol $Py \cdot m^{-2}$) or Pt(1.7)/SiO_2 (0.061 μmol $Py \cdot m^{-2}$), avoids the formation of heavy products that leads to a fast deactivation. The catalysts that have high acid sites density, e.g., Pt(1.7)/H-Beta zeolite (1.545 μmol $Py \cdot m^{-2}$), favor the condensation of coke precursors adsorbed on adjacent sites. The effect of acidity on coke formation and gasification was also addressed in this previous study.[28]

Using the dispersion previously determined[15] and the number of acid sites measured by pyridine TPD, the metal/acid sites ratio (M/A) was calculated for all the catalysts. The values obtained were 0.922, 0.324, 0.065, and 0.035 for the catalysts containing 1.7, 0.5, 0.1, and 0.05 wt % Pt, respectively.

3.2. Deactivation of Bifunctional Pt/Al_2O_3 Catalyst.

Deactivation Mechanism. The reaction routes for cresol deoxygenation shown in Scheme 1 involve metallic and acid functions.[15] Results obtained without catalyst showed that the thermal conversion of cresol was negligible at 500 °C (results not shown). In the presence of catalyst, toluene is formed by dehydroxylation of cresol. It has been proposed that this reaction occurs on the metal after the aromatic ring is partially hydrogenated, and then the C−O bond breakage occurs, followed by dehydrogenation of the ring.[29,30] Phenol is formed by hydrogenolysis of the cresol methyl group. Two different routes generate benzene. Hydrogenolysis of toluene methyl group produces benzene and methane, while dehydroxylation of phenol forms benzene. Methylcyclohexane was formed by hydrogenation of toluene. Other products found by GC−MS in low amounts were dimethyldiphenyl and dimethylbenzophenone. Methyl groups from these compounds can be hydrocracked, and because of this, the light hydrocarbon fraction (which contained an important amount of methane) yield was higher than the benzene yield.

Scheme 1. Reaction Routes for *m*-Cresol Deoxygenation over Pt/γAl_2O_3

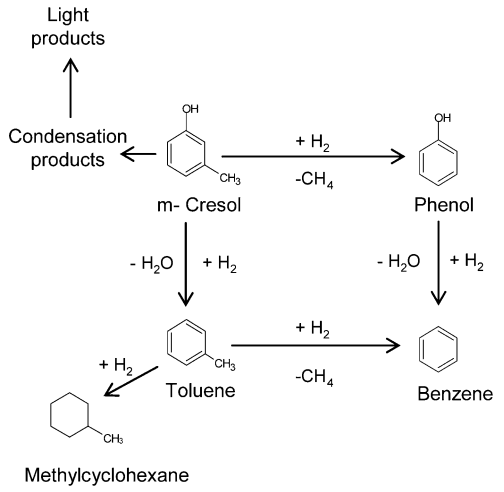

During the reaction of cresol deoxygenation, both the metallic and the acid functions deactivate by coke formation, although the amount of coke on the support increases faster than on the metal, as demonstrated by Zanuttini et al. by TPO analysis of coked catalysts.[15]

As a result, the selectivity to "light products", formed by the hydrocracking of condensation products over the acid functions, decreased. On the other hand, since the toluene formation depends more strongly on the metallic function, its selectivity increased as catalyst deactivation occurred.

Figure 1 shows the TPO profiles of Pt(1.7)/γ-Al_2O_3 catalyst after reactions carried out at two different H_2/*m*-cresol molar ratio and at different contact times. The activity data corresponding to these results have already been presented.[15] It can be observed that the contact time used during the reaction led to important changes in the coke amount and characteristics. Two regions in the TPO profile can be clearly distinguished. The first one is related to the coke that is deposited on the metal particles or in the vicinity of these particles and is represented by the well-defined peak that appears in the 200−250 °C range. It has been well established that for Pt/γ-Al_2O_3 catalysts, this peak corresponds to the coke

DOI: 10.1021/acs.iecr.5b00305
Ind. Eng. Chem. Res. XXXX, XXX, XXX−XXX

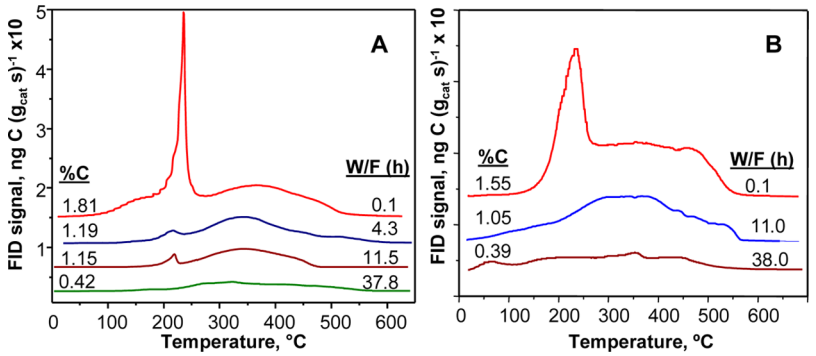

Figure 1. TPO profiles for different contact times (W/F), with catalyst Pt(1.7)/γAl_2O_3, reaction at 300 °C: (A) H_2/*m*-cresol molar ratio of 197; (B) H_2/*m*-cresol molar ratio of 510. Time on stream is 390 min.

on or near the metal particles.[31−33] The coke that gasified in the 250−500 °C temperature range is deposited on the support.

When pure alumina was tested, the *m*-cresol conversion was negligible. The amount of coke deposited was 12%, significantly higher than on Pt(0.05)/Al_2O_3 under the same conditions, with a maximum in the TPO profile at 490 °C. The presence of the metallic function, even at very low concentration, not only changes the relative rates of the reactions involved in this system but also generates hydrogen spillover leading to an important improvement in the catalyst stability.[15]

As the residence time (W/F) decreased, the conversion also decreased,[15] and consequently there was a higher *m*-cresol composition along the catalyst bed. It can be observed in Figure 1 that the lower is the (W/F), the higher is the amount of coke deposited on the catalyst. Therefore, these results show that the deactivation occurs by a parallel mechanism, in which the coke is formed faster from the reactant than from the products. Similar type of deactivation mechanism, i.e., with a decrease in coke content as the W/F increases, was observed in the alkylation of isobutane with butenes,[34] in *n*-heptane re-forming on nonsulfided Pt−Re/Al_2O_3,[35] in the case of methanol to olefins conversion,[36] and in ethanol dehydration on zeolites.[37]

According to results shown in Figure 1, there is a strong effect of the oxygenated compound composition in the rate of coke formation on the metal particles or close to them. It can be observed that the first peak in the TPO profiles decreased very quickly as the W/F increased. Similar results were obtained using two H_2/*m*-cresol ratios (compare Figure 1A and Figure 1B).

To demonstrate that the coke formation mechanism above proposed is correct, an additional experiment was performed. The reactor was prepared in order to have the catalyst separated in three consecutive beds using quartz wool. The global W/F used was 0.3 $g_{cat}\cdot h\cdot(g_{cresol})^{-1}$. H_2/cresol molar ratio was 64, and the reaction duration was 12 h. After reaction, the TPO profile and %C were obtained for each part of bed. Figure 2 shows the results and a photo of the reactor after the reaction. The values of %C obtained for the top, middle, and bottom parts were 10.3%, 7.5%, and 6.9%, respectively. The top part of the bed, at the beginning of the reactor, with the shorter residence time and the highest concentration of *m*-cresol was the one with the highest coke content, while the bottom part with the highest concentration of products and the lowest of *m*-cresol was the one with the lowest coke value. These results also indicate that coke formation follows a parallel mechanism, the *m*-cresol being the main precursor.

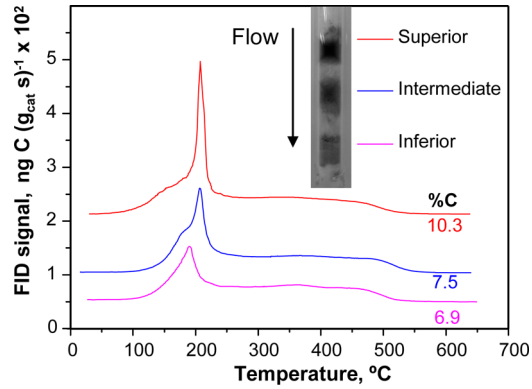

Figure 2. TPO profiles for coked catalysts, at different bed positions: catalyst, Pt(1.7)/γ-Al_2O_3, reaction at 300 °C; W/F = 0.3 $g_{cat}\cdot h\cdot(g_{cresol})^{-1}$; H_2/*m*-cresol molar ratio of 64. Time on stream is 660 min.

After each reaction test a carbon balance was calculated as described in section 2.3. For instance, assuming that all the "light products" were represented by methane, in a standard reaction of 160 min at 300 °C, W/F = 37.7 $g_{cat}\cdot h\cdot(g_{cresol})^{-1}$, H_2/cresol = 510, with 30% of light products, and the C recovery calculated was 90%. However, since other compounds with higher number of C atoms were present, the C loss was well bellow 10%. With the same calculation procedure for a reaction under the same conditions but using W/F = 0.06 $g_{cat}\cdot h\cdot(g_{cresol})^{-1}$ the recovery of C was 97%.

3.3. Effect of the H_2/Cresol Ratio on Coke Deposition.

Figure 3 shows the TPO profiles and the amounts of coke deposited during the *m*-cresol deoxygenation reaction at different H_2/cresol ratios and two residence times.

Figure 3A shows that at a residence time (W/F) of 6.4 $g_{cat}\cdot h\cdot(g_{cresol})^{-1}$, the higher is the H_2/cresol ratio, the lower is the total amount of coke deposited. On the other hand, as the hydrogen concentration increased, a pronounced effect on the coke related to the metal particles was observed. At H_2/cresol ratios above 250 the first peak in the TPO profile was hardly distinguished, while there was a small amount of coke deposited on the acid function. This means that the hydrogen partial pressure has a direct effect on the kinetics of the different reactions involved in the mechanism shown in Scheme 1 and also an indirect effect due to the different coke deposition rates on each active function, with a more pronounce effect on the coke amount formed on the metal particles.

Figure 3 B shows similar results, obtained at a lower residence time (0.1 $g_{cat}\cdot h\cdot(g_{cresol})^{-1}$) than that used in the experiments shown in Figure 3A. The lower residence time

DOI: 10.1021/acs.iecr.5b00305
Ind. Eng. Chem. Res. XXXX, XXX, XXX−XXX

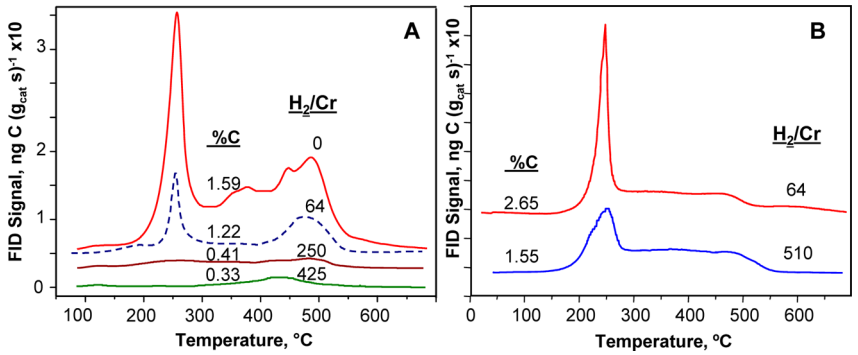

Figure 3. TPO profiles and the amounts of coke on the catalyst for different H_2/cresol ratios, with catalyst Pt(1.7)/γ-Al_2O_3, reaction at 300 °C: (A) W/F = 6.4 $g_{cat}\cdot h\cdot(g_{cresol})^{-1}$; (B) W/F = 0.1 $g_{cat}\cdot h\cdot(g_{cresol})^{-1}$.

corresponds to reaction conditions that led to lower conversions, and consequently, there was a higher *m*-cresol concentration along the catalyst bed. Under these conditions, even at high H_2/cresol ratios, there was an appreciable amount of coke deposited on or near the metal particles.

3.4. Effect of Pt Loading on Product Distribution and Deactivation. The product distribution was studied with catalysts containing Pt loadings between 0.05 and 1.7 wt %. Figure 4 shows the product yields for different Pt loadings and the *same m-cresol conversion*, and Table 1 shows the amounts of coke deposited on each catalyst during these experiments. Figure 4 shows that the selectivity to different products changed significantly with the Pt loading, even though the total *m*-cresol conversion was the same. The higher Pt loading favors the deoxygenation reaction giving toluene as the main product. Although acid sites are required for this reaction, the limiting step is controlled by the metal function, as indicated by the results shown in Figure 4 and also as previously proposed.[15] This means that a high Pt loading, e.g., 1.7 wt % leads to a fast formation of toluene, which has a low coke-forming tendency. On the other hand, with low Pt loading, e.g., 0.05 wt %, the toluene formation is slow, thus favoring the formation of "light products", which are formed by cracking of heavy products formed by condensation on acid sites. These results indicate that the ratio between the amount of metallic sites and acid sites strongly affects the products distribution and coke formation, as shown in Table 1. The *m*-cresol deoxygenation is controlled by the metal function, but the mechanism involves a dehydration step on the acid sites of the partially hydrogenated phenolic ring. On the other hand, the formation of light products occurs on the acid sites but requires hydrogen that reaches the condensation products by spillover after adsorption on the metallic particle. These bifunctional reactions compete in this system, the ratio of metal/acid functions being the parameter that makes it possible to favor one of these reactions routes. Table 1 shows the residence time referenced to Pt, calculated as the mass of Pt loaded in the reactor divided by the *m*-cresol flow rate. This value was exactly the same, within experimental errors, for the four catalysts. This means that the total conversion is controlled by the amount of Pt loaded in the reactor, and that the product distribution is controlled by the metal/acid sites ratio, as previously stated.[15]

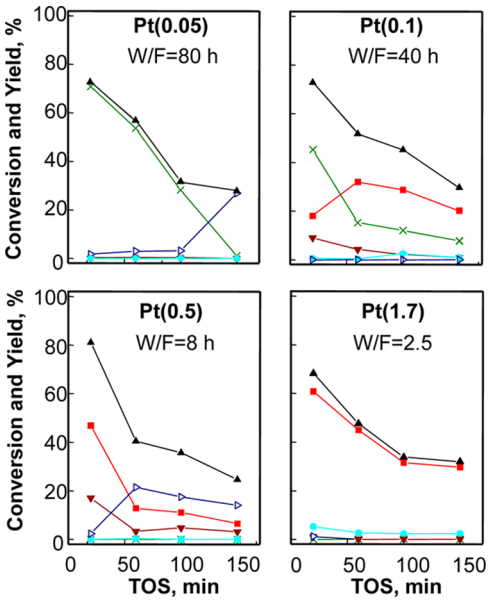

Figure 4. *m*-Cresol conversion and product yields vs time on stream (TOS) for the different Pt/γ-Al_2O_3 catalysts, at 300 °C, H_2/*m*-cresol molar ratio of 1483. Reference: (▲) *m*-cresol conversion. Yields: (■) toluene, (×) light products, (▼) benzene, (▷) phenol, and (●) methylcyclohexane.

Figure 5 shows the TPO profiles obtained with catalysts containing different Pt loadings, from 0.05 to 1.7 wt %, corresponding to the experiments in which the conversion was the same for all the catalysts (experiments shown in Figure 4

Table 1. Reaction Conditions Used To Compare the Cataysts with Different Pt Content under Similar Conversion Levels[a]

Pt, %	H_2, mL min^{-1}	W, mg	cresol molar fraction (10^3)	W/F, $g_{cat}\cdot h\cdot g_{cresol}^{-1}$	W_{Pt}/F, $mg_{Pt}\cdot h\cdot g_{cresol}^{-1}$	%C
0.05	7	100.0	4.72	79.9	40.0	1.30
0.10	7	50.0	4.72	40.0	40.0	5.30
0.50	15	20.0	10.11	7.5	37.5	5.47
1.70	30	13.2	20.22	2.5	42.5	2.44

[a]Partial pressure of cresol: 6.7×10^{-4} atm. H_2/cresol molar ratio of 1483.6. Temperature of 40°C. W: catalyst mass. W_{Pt}: mass of Pt in the catalyst loaded in the reactor.

DOI: 10.1021/acs.iecr.5b00305
Ind. Eng. Chem. Res. XXXX, XXX, XXX−XXX

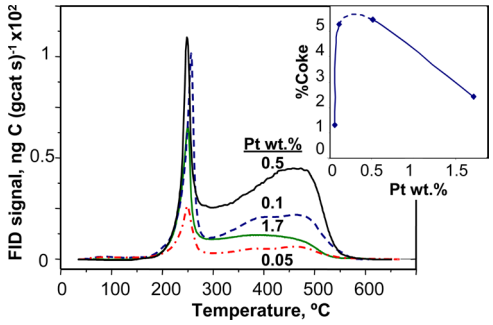

Figure 5. TPO profiles for the different Pt/γ-Al_2O_3 catalysts after 136 min of reaction at 300 °C, with H_2/*m*-cresol molar ratio of 1483. Insert: %C vs Pt content.

and Table 1). The amount of coke that corresponds to each of them is shown in Table 1. As shown in Figures 1, 2, and 3, the TPO profiles display a peak below 300 °C that is characteristic of coke deposited on or near the metal particles and was observed with the four catalysts. The insert in Figure 5 shows the variation of the coke content on each catalyst as a function of the Pt content. It can be observed that there is a maximum in this curve, with a low amount of coke deposited on the catalysts containing 0.05 and 1.7 wt % Pt and higher amounts of coke for catalysts with 0.1 and 0.5 wt % Pt. These results clearly demonstrate the strong dependency of the amount of coke on the metal content. Coke is mostly formed from cresol, as inferred from the results obtained at different contact times; however, the other compounds present in the system also form coke, e.g., toluene and benzene. It is well-known that in the presence of Pt/γ-Al_2O_3 re-forming catalysts, coke formation is produced by mechanism involving both the metallic and the acid functions.[38,39] According to the results shown in Figure 5 and the products distribution shown in Figure 4, at high Pt content there is a fast formation of toluene, which is a compound that has a low tendency to form coke. On the other hand, at very low Pt content (0.05 wt %) the hydrogenation/dehydrogenation activity is extremely low. As a consequence, the first step in the coke formation mechanism, which is a partial ring hydrogenation,[38,39] occurs at a low rate and a low amount of coke is formed on the catalyst.

3.5. Coke Formation Mechanism. Scheme 2 shows a simplified coke formation mechanism, based on the results shown in previous sections and in several studies reported by other research groups. In the case of the Pt(0.05) catalyst that has the lowest metal/acid sites ratio (M/A = 0.035), the main reaction path is the formation of a surface pool of condensation products that are hydrocracked forming light compounds, as previously proposed by Ausavasukhi et al.[16] In this case, a very low amount of coke is formed, as shown in Figure 5. In the presence of metal, the cresol is partially hydrogenated, and then the OH is eliminated either by dehydration on the acid sites[29,30] or by hydrodeoxygenation on the metal sites,[40] forming toluene in both cases. The partially dehydrogenated compounds, represented in Scheme 2 by a cyclohexadiene substituted compound, are highly reactive in the presence of acid sites, forming methylcyclopentenes and methylcyclopentadienes, which by Diels–Alder condensation led to the formation of coke.[31−33] However, these partially dehydrogenated intermediates can be easily transformed in toluene in the presence of high Pt loading, competing with the coke formation reaction, and under this condition, forming lower amount of coke as shown in Figure 5 for Pt(1.7)/γ-Al_2O_3. As indicated in Scheme 2, the formation of toluene and coke occurs by parallel reactions, with a faster coke formation as the cresol concentration in the reaction media increases. Similar analysis can be done starting from phenol.

Scheme 2 also shows how the metal/acid sites ratio affects products distribution. At very low M/A ratio such as that of Pt(0.05)/γ-Al_2O_3 (M/A = 0.035), the main reaction path is the formation of light products, while at high M/A ratio the formation of toluene is largely favored, as shown in Figure 4 for Pt(1.7)/γ-Al_2O_3 (M/A = 0.922). Pt(0.5) and Pt(0.1) have intermediates values of M/A ratios (0.32 and 0.035, respectively), and in these cases the selectivities to benzene, phenol, and coke are higher than in the other two cases.

It is a very interesting result, the fact that even with a very low amount of Pt, e.g., 0.05 wt %, the catalytic behavior exhibits a dramatic change, decreasing the coke deposition from 12% in bare alumina to 1.3 wt % in Pt(0.05). As indicated in Scheme 2, the formation of light products from the surface pool of condensation products requires H_2, which is provided by spillover promoted by Pt, even if it is present in low loadings.

Scheme 2. Simplified Deactivation Mechanism

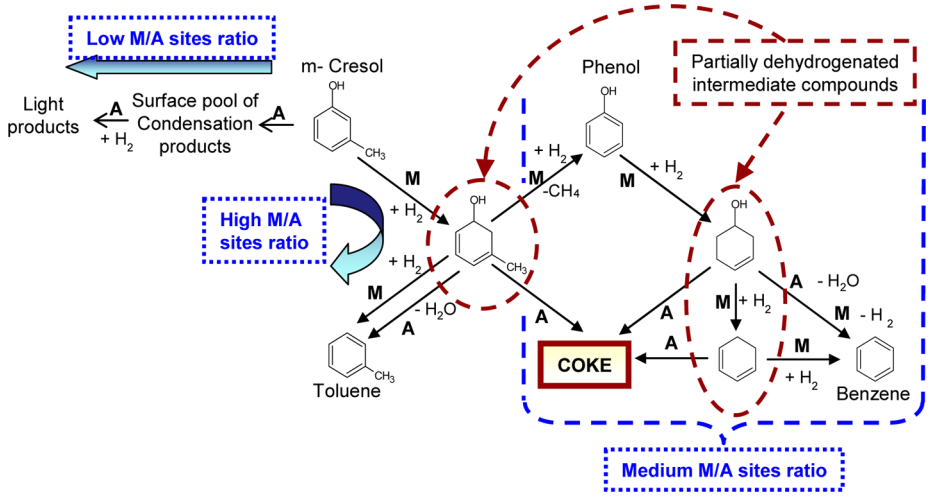

DOI: 10.1021/acs.iecr.5b00305
Ind. Eng. Chem. Res. XXXX, XXX, XXX−XXX

3.6. Regeneration. Different regeneration treatments, using H_2 or air, were performed.

3.6.1. Regeneration with Air. Figure 6 shows the conversion and products yields before and after the treatment in air at 350 °C. The catalytic activity was successfully recovered after this treatment. A TPO profile of the spent catalyst treated with air at 350 °C during 1 h, i.e., with the same treatment as that used during the regeneration, showed that the coke that corresponds to the low temperature peaks was completely eliminated, as shown in Figure 7A, but a small amount of coke remained on the acid sites, as observed by the TPO signals evolved at high temperatures between 400 and 550 °C. Therefore, the regeneration treatment used in this experiment led to a change in the metal/acid sites ratio, since coke was fully removed from the metal particles, and a small amount was left on the support, thus increasing the effective M/A sites ratio. This change in the metal/acid ratio explains the small increase observed in the selectivity toward toluene formation, as shown in Figure 6. As the metal/acid ratio increased after the regeneration step, the toluene/light compounds ratio also increased, as above-discussed and as experimentally found (Figure 6). A very important conclusion obtained from this study is that it is not necessary to completely regenerate both catalytic functions and that the regeneration of the metallic function is a key factor to regenerate the catalyst with air. In this way, higher temperature can be avoided during regeneration, thus preserving the platinum dispersion.

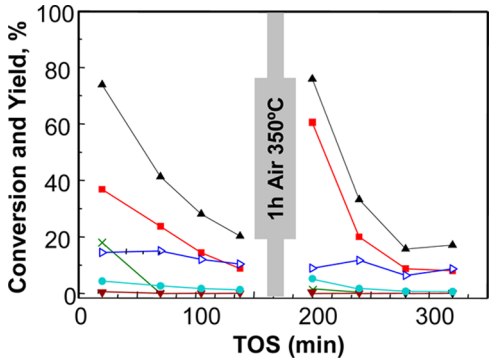

Figure 6. *m*-Cresol conversion and product yields vs time on stream (TOS) before and after regeneration with air at 350 °C, Pt (1.7%)/γ-Al_2O_3, 300 °C, W/F = 0.08 $g_{cat}\cdot h\cdot(g_{cresol})^{-1}$, H_2/*m*-cresol molar ratio of 64. Reference: (▲) *m*-cresol conversion. Yields: (■) toluene, (×) light products, (▼) benzene, (▷) phenol, and (●) methylcyclohexane.

The particle size distribution was determined after the treatment with air at 350 °C, and it was found that the mean size did not change, maintaining the value of 1.5 nm. Figure 7B shows the histograms of the particle sizes for the fresh catalyst, the catalyst after treatment with air at 350 °C, and the catalyst after a treatment with H_2 at 500 °C. Although the variation in the average particle size is small, it can be observed that the distribution is slightly different; there are more particles of higher diameter and also more particles of smaller diameter, compared to the fresh catalyst.

XPS results obtained with the fresh Pt(1.7)/γ-Al_2O_3 catalyst and after treatment with air and activation at 500 °C are presented in Table 2. The decomposition of the spectral region of the Pt $4d_{5/2}$ line with subtraction of a Shirley background spectrum of fresh and regenerated Pt(1.7)/γ-Al_2O_3 to individual components revealed the presence of two platinum states: the reduced state (Pt^0) with a binding energy (Eb) of 314.0−314.2 eV and the oxidized state with a Eb of 316.9−317 eV. Table 2 presents the Pt $4d_{5/2}$ binding energies and the percentages of the different states of platinum. These results show that there were no significant differences between the fresh and the regenerated catalyst. The signals in the region of O 1s were also very similar. However, the area under the signal of C 1s for the used and regenerated catalyst was higher than the one observed for the fresh catalyst, indicating a higher amount of C on the surface of the catalyst. These results agree with those observed by TPO where, after the regeneration process, the catalyst still showed a certain amount of carbonaceous deposits.

Table 2. XPS Results Obtained with the Fresh and the Regenerated Catalyst

	catalyst	
	fresh	after regeneration with air
binding energy Pt $4d_{5/2}$ (eV)	314.1	314.2
	317.0	317.0
% Pt^0	54.7	55.2
% PtO_x	45.3	44.8

3.6.2. Regeneration in Hydrogen. It should be recalled that after treatment of the used catalyst with air, platinum particles were partially oxidized, so it was necessary to perform activation

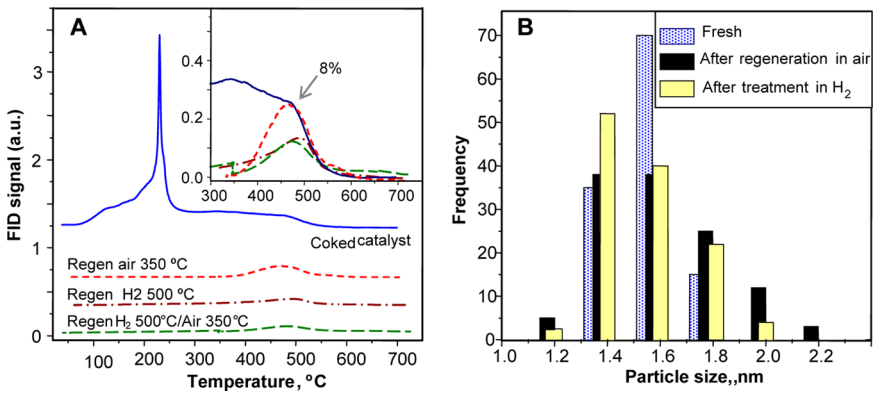

Figure 7. (A) TPO profiles for the Pt(1.7)/γ-Al_2O_3 after 136 min of reation at 300 °C, H_2/*m*-cresol molar ratio of 64. (B) TEM results of fresh and regenerated catalysts: histograms of Pt(1.7)/γ-Al_2O_3.

DOI: 10.1021/acs.iecr.5b00305
Ind. Eng. Chem. Res. XXXX, XXX, XXX−XXX

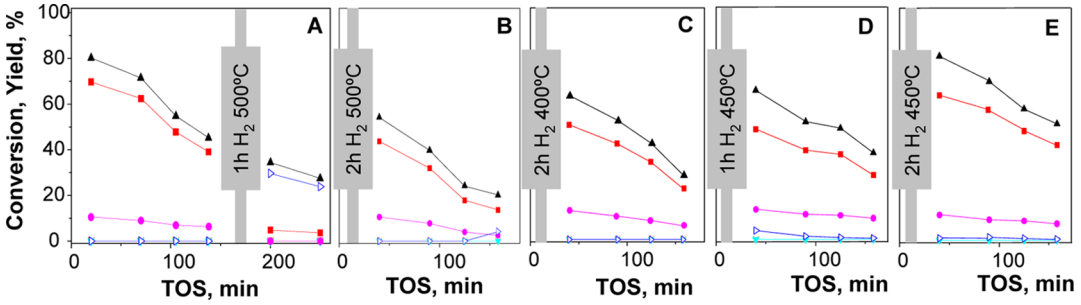

Figure 8. *m*-Cresol conversion and product yields vs time on stream (TPO) for Pt (1.7%)/γ-Al_2O_3, 300 °C, W/F = 0.08 $g_{cat}\cdot h\cdot(g_{cresol})^{-1}$, H_2/*m*-cresol molar ratio of 111: (A) before and after treatment for 1 h with H_2 at 500 °C; (B) after treatment for 2 h with H_2 at 500 °C; (C) after treatment for 2 h with H_2 at 400 °C; (D) after treatment for 1 h with H_2 at 450 °C; (E) after treatment for 2 h with H_2 at 450 °C. Reference: (▲) *m*-cresol conversion. Yields: (■) toluene, (×) light products, (▼) benzene, (▷) phenol, and (●) methylcyclohexane.

in H_2 at 500 °C. In order to simplify the process of regeneration and to avoid introducing air into the system, direct regeneration using hydrogen was studied. The idea is to promote the hydrogenolysis and hydrocracking of condensation products using hydrogen at a temperature higher than the reaction temperature.

Figure 8 shows the results obtained before and after H_2 treatment at different temperatures and times. It is very interesting to observe that the regenerability in hydrogen has a complex dependence with these variables. At a regeneration temperature of 500 °C it was not possible to recover the initial catalytic behavior, with a very poor performance when the regeneration treatment was carried out only for 1 h (Figure 8A). In this case, neither the activity nor the selectivity to toluene was recovered. At 400 °C, the regeneration was even better than at 500 °C after 2 h of treatment (Figure 8B and Figure 8C). Finally, the best result was obtained at 450 °C, being necessary to maintain this temperature for 2 h in order to fully recover the activity and selectivity (Figure 8E). Foster et al.[17] found that it was possible to regenerate the catalyst with hydrogen at 450 °C but did not present results obtained at other regeneration temperatures. Figure 7A shows the TPO profile obtained after treatment in H_2 at 500 °C. Although most of the coke was removed, conversion was not recovered and phenol was the main product observed after the regeneration, as shown in Figure 8A. This means that the high temperature treatment in hydrogen led to the formation of a coke with high toxicity, decreasing the activity of the acid function in such a way that the catalyst loses the activity for the dehydration step that is needed in order to obtain toluene. In addition, the high selectivity to phenol observed in this case suggests that there was a drastic decrease in the M/A sites ratio due to the coke left on the catalyst during this regeneration. In the inset of Figure 7A, it can be observed that the temperature needed to remove the coke left on the catalyst after the treatment with hydrogen at 500 °C during 1 h is slightly higher than that needed to remove the coke left after the treatment with air at 350 °C. This means that during the treatment at 500 °C, the nonremoved coke is transformed to a more toxic residue because of aromatization reactions that occur on the acid sites, as was observed also in alkylation catalysts.[30] According to the activity results, which show a lower *m*-cresol conversion and a high selectivity to phenol indicating a decrease in the availability of metal sites, the presence of a small amount of coke on the metal particles is very likely, although not being possible to be detected by TPO. This indicates that treatment with hydrogen at high temperature leads to the formation of carbonaceous deposits with high toxicity, thereby decreasing the activity of the sites such that the catalyst loses its ability to promote the dehydration step, necessary for toluene formation.

On the other hand, when a low temperature such as 400 °C was used for the regeneration in hydrogen for 2 h, a larger fraction of coke was left on the catalyst as it is observed in Figure 9 (line b), and because of this, it was not possible to fully

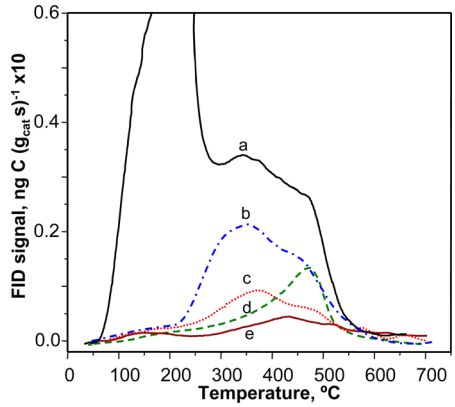

Figure 9. TPO profiles for the Pt(1.7)/γ-Al_2O_3 after 136 min of reation at 300 °C, H_2/*m*-cresol molar ratio of 111: (a) coked catalyst, without any regeneration treatment; (b) after treatment in H_2, 2 h at 400 °C; (c) after treatment in H_2, 2 h at 450 °C; (d) after treatment in H_2, 1 h at 500 °C; (e) after treatment in H_2, 2 h at 500 °C.

recover the activity. At an intermediate temperature of 450 °C and time of 2 h, it is possible to remove most of the coke without changing the toxicity of the fraction left on the catalyst (Figure 9, line c).

3.6.3. Combined Regeneration with Hydrogen and Air. Additional experiments were carried out with the objective of verifying the reasons for the change of selectivity after hydrogen treatment at 500 °C. After 136 min of reaction, the spent catalyst was first treated with H_2 during 1 h at 500 °C and then with air at 350 °C. The results are shown in Figure 10A. After this procedure, the catalyst did not recover the conversion but the selectivity to toluene was maintained. The TPO profile of the coke that remained on the catalyst after the combined treatment of hydrogen and air is shown in Figure 7A. It can be observed that only a very small amount of coke was left on the catalyst, mainly on the acid function, but as above-mentioned, the activity results suggest that a very small amount of coke is also present on the metal particles. Nevertheless, when a similar experiment was performed, but treating the deactivated catalyst

DOI: 10.1021/acs.iecr.5b00305
Ind. Eng. Chem. Res. XXXX, XXX, XXX−XXX

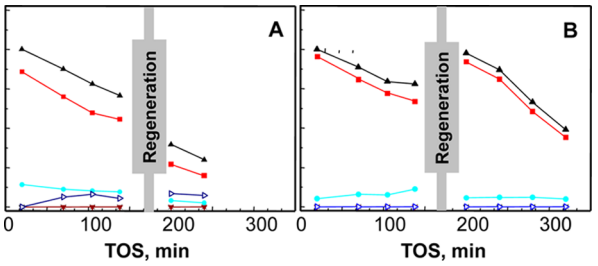

Figure 10. *m*-Cresol conversion and product yields vs time on stream (TOS) for Pt (1.7%)/γ-Al_2O_3, 300 °C, W/F = 0.08 $g_{cat}\cdot h\cdot(g_{cresol})^{-1}$, H_2/*m*-cresol molar ratio of 111: (A) before and after treatment in H_2 at 500 °C and air at 350 °C; (B) before and after treatment in H_2 at 500 °C and air at 500 °C. Reference: (▲) *m*-cresol conversion. Yields: (■) toluene, (×) light products, (▼) benzene, (▷) phenol, and (●) methylcyclohexane.

for 1 h in H_2 at 500 °C and then for 30 min in air at 500 °C, both the selectivity and the conversion were completely recovered (Figure 10B). The TPO profile obtained after this treatment (not shown) indicated that the coke was completely removed from the catalyst.

This set of experiments makes it possible to conclude that the deactivation was due mainly to coke deposition and that it is possible to recover the catalytic activity and selectivity by removing the coke with air at mild temperatures, such as 350 °C, or with hydrogen at 450 °C. The latter should be the preferred regeneration treatment, since it does not require changing gases for each step of the process, i.e., reaction and regeneration.

4. CONCLUSIONS

The Pt/γ-Al_2O_3 is an active catalyst for cresol deoxygenation. The metal loading has a strong influence in the product distribution because as the ratio of metal/acid sites increases, the toluene formation is favored. This also has important effects on the amount of coke deposited on the catalyst. The total amount of coke shows a maximum as a function of the platinum content. At low loading, the dehydrogenating activity is too low, and the coke precursors formation is correspondingly low. At high platinum content, there is a fast formation of toluene, which has a low tendency to form coke. An important finding is that in order to obtain similar conversion between catalysts with different platinum content, the same residence time referenced to the Pt content must be used. This demonstrated that the metal is controlling the cresol conversion, while the metal/acid sites ratio controls the selectivity and coke formation rate. Coke is deposited on both functions, a treatment with air at mild temperatures being necessary in order to remove the coke and recover the activity and selectivity. The regeneration in hydrogen is possible at 450 °C if enough time is used in this procedure, but it is not possible at 400 or at 500 °C either because not enough amount of coke is removed or because the toxicity of the low fraction of coke left on the catalyst is too high.

AUTHOR INFORMATION

Corresponding Author

*E-mail: querini@fiq.unl.edu.ar. Tel: +54-342-4533858. Fax: +54-342-4531068.

Notes

The authors declare no competing financial interest.

ACKNOWLEDGMENTS

The authors acknowledge the financial support received from CONICET (Grant PIP 2010-093), UNL (Grant PACT 69), and ANPCyT (Grant PICT 2010-1526).

REFERENCES

(1) Sheu, Y.-H. E.; Anthony, R. G.; Soltes, E. J. Kinetic studies of upgrading pine pyrolytic oil by hydrotreatment. *Fuel Process. Technol.* **1988**, *19*, 31−50.

(2) Baker, E. G.; Elliott, D. C. Catalytic Upgrading of Biomass Pyrolysis Oils. In *Research in Thermochemical Biomass Conversion*; Bridgwater, A. V., Kuester, J. L., Eds.; Springer: Dordrecht, The Netherlands, 1988; pp 883−895.

(3) Agblevor, F.; Besler, S. Inorganic compounds in biomass feedstocks. 1. Effect on the quality of fast pyrolysis oils. *Energy Fuels* **1996**, *10*, 293−298.

(4) Craig, W.; Coxworth, E. Conversion of vegetable oils to conventional liquid fuel extenders. *Sixth Canadian Bioenergy R&D Seminar*, Proceedings, Richmond, Canada, 1987; Elsevier Applied Science: London, 1987; pp 407−411.

(5) Maggi, R.; Delmon, B.; Bridgwater, A. *Advances in Thermochemical Biomass Conversion*; Elsevier Applied Science: London, 1993.

(6) Maggi, R.; Centeno, A.; Delmon, B. Biomass Energy Environ. *Proceedings of the 9th European Bioenergy Conference*; Elsevier: Oxford, U.K., 1996; pp 327.

(7) Grange, P.; Laurent, E.; Maggi, R.; Centeno, A.; Delmon, B. Hydrotreatment of pyrolysis oils from biomass: reactivity of the various categories of oxygenated compounds and preliminary techno-economical study. *Catal. Today* **1996**, *29*, 297−301.

(8) Fisk, C. A.; Morgan, T.; Ji, Y.; Crocker, M.; Crofcheck, C.; Lewis, S. A. Bio-oil upgrading over platinum catalysts using in situ generated hydrogen. *Appl. Catal., A* **2009**, *358*, 150−156.

(9) Wang, W.; Yang, Y.; Luo, H.; Hu, T.; Liu, W. Amorphous Co−Mo−B catalyst with high activity for the hydrodeoxygenation of bio-oil. *Catal. Commun.* **2011**, *12*, 436−440.

(10) Adjaye, J.; Bakhshi, N. Production of hydrocarbons by catalytic upgrading of a fast pyrolysis bio-oil. Part I: Conversion over various catalysts. *Fuel Process. Technol.* **1995**, *45*, 161−183.

(11) Katikaneni, S. P.; Adjaye, J. D.; Idem, R. O.; Bakhshi, N. N. Catalytic conversion of canola oil over potassium-impregnated HZSM-5 catalysts: C2-C4 olefin production and model reaction studies. *Ind. Eng. Chem. Res.* **1996**, *35*, 3332−3346.

(12) Williams, P. T.; Horne, P. A. The influence of catalyst regeneration on the composition of zeolite-upgraded biomass pyrolysis oils. *Fuel* **1995**, *74*, 1839−1851.

(13) Adjaye, J.; Bakhshi, N. Production of hydrocarbons by catalytic upgrading of a fast pyrolysis bio-oil. Part II: Comparative catalyst performance and reaction pathways. *Fuel Process. Technol.* **1995**, *45*, 185−202.

(14) Janssen, F., Catalysis for renewable energy and chemicals: The thermal conversion of biomass. In *Environmental Catalysis*; Janssen, F. J. J. G., van Santen, R. A., Eds.; Imperial College Press: London, 1999; pp 15−36.

(15) Zanuttini, M.; Lago, C.; Querini, C.; Peralta, M. Deoxygenation of m-cresol on Pt/γ-Al_2O_3 catalysts. *Catal. Today* **2013**, *213*, 9−17.

(16) Ausavasukhi, A.; Huang, Y.; To, A. T.; Sooknoi, T.; Resasco, D. E. Hydrodeoxygenation of m-cresol over gallium-modified beta zeolite catalysts. *J. Catal.* **2012**, *290*, 90−100.

(17) Foster, A. J.; Do, P. T.; Lobo, R. F. The synergy of the support acid function and the metal function in the catalytic hydrodeoxygenation of m-cresol. *Top. Catal.* **2012**, *55*, 118−128.

(18) Do, P. T.; Chiappero, M.; Lobban, L. L.; Resasco, D. E. Catalytic deoxygenation of methyl-octanoate and methyl-stearate on Pt/Al_2O_3. *Catal. Lett.* **2009**, *130*, 9−18.

(19) Aben, P. Palladium areas in supported catalysts: determination of palladium surface areas in supported catalysts by means of hydrogen chemisorption. *J. Catal.* **1968**, *10*, 224−229.

DOI: 10.1021/acs.iecr.5b00305
Ind. Eng. Chem. Res. XXXX, XXX, XXX−XXX

(20) White, M. G. *Heterogeneous Catalysis*; Prentice Hall: Upper Saddle River, NJ, U.S., 1990.
(21) Fung, S.; Querini, C. A highly sensitive detection method for temperature programmed oxidation of coke deposits: Methanation of CO_2 in the presence of O_2. *J. Catal.* **1992**, *138*, 240−254.
(22) Benson, J.; Hwang, H.; Boudart, M. Hydrogen-oxygen titration method for the measurement of supported palladium surface areas. *J. Catal.* **1973**, *30* (1), 146−153.
(23) Meephoka, C.; Chaisuk, C.; Samparnpiboon, P.; Praserthdam, P. Effect of phase composition between nano γ-and χ-Al_2O_3 on Pt/Al_2O_3 catalyst in CO oxidation. *Catal. Commun.* **2008**, *9*, 546−550.
(24) Tiernan, M. J.; Finlayson, O. E. Effects of ceria on the combustion activity and surface properties of Pt/Al_2O_3 catalysts. *Appl. Catal., B* **1998**, *19*, 23−35.
(25) Santos, A. C. S. F.; Damyanova, S.; Teixeira, G. N. R.; Mattos, L. V.; Noronha, F. B.; Passos, F. B.; Bueno, J. M. C. The effect of ceria content on the performance of $Pt/CeO_2/Al_2O_3$ catalysts in the partial oxidation of methane. *Appl. Catal., A* **2005**, *290*, 123−132.
(26) Serrano-Ruiz, J. C.; Huber, G. W.; Sánchez-Castillo, M. A.; Dumesic, J. A.; Rodríguez-Reinoso, F.; Sepúlveda-Escribano, A. Effect of Sn addition to Pt/CeO_2−Al_2O_3 and Pt/Al_2O_3 catalysts: An XPS, ^{119}Sn Mössbauer and microcalorimetry study. *J. Catal.* **2006**, *241*, 378−388.
(27) Ivanova, A. S.; Slavinskaya, E. M.; Gulyaev, R. V.; Zaikovskii, V. I.; Stonkus, O. A.; Danilova, I. G.; Plyasova, L. M.; Polukhina, I. A.; Boronin, A. I. Metal−support interactions in Pt/Al_2O_3 and Pd/Al_2O_3 catalysts for CO oxidation. *Appl. Catal., B* **2010**, *97*, 57−71.
(28) Zanuttini, M.; Dalla Costa, B.; Querini, C.; Peralta, M. Hydrodeoxygenation of m-cresol with Pt supported over mild acid materials. *Appl. Catal., A* **2014**, *482*, 352−361.
(29) Do, P. T. M.; Foster, A. J.; Chen, J.; Lobo, R. F. Bimetallic effects in the hydrodeoxygenation of meta-cresol on gamma-Al_2O_3 supported Pt-Ni and Pt-Co catalysts. *Green Chem.* **2012**, *14*, 1388−1397.
(30) Taylor, D. R.; Ludlum, K. H. Structure and orientation of phenols chemisorbed on gamma-alumina. *J. Phys. Chem.* **1972**, *76*, 2882−2886.
(31) Barbier, J.; Churin, E.; Marecot, P. Coking of $Pt\text{-}Ir/Al_2O_3$ and $Pt\text{-}Re/Al_2O_3$ catalysts in different pressures of cyclopentane. *J. Catal.* **1990**, *126*, 228−234.
(32) Barbier, J. Coking of Reforming Catalysts. In *Studies in Surface Science and Catalysis*; Delmon, B., Froment, G. F., Eds.; Elsevier: Amsterdam, 1987; Vol. *34*, pp 1−19.
(33) Barbier, J.; Churin, E.; Parera, J. M.; Riviere, J. Characterization of coke by hydrogen and carbon analysis. *React. Kinet. Catal. Lett.* **1985**, *29*, 323−330.
(34) Querini, C.; Roa, E. Deactivation of solid acid catalysts during isobutane alkylation with C4 olefins. *Appl. Catal., A* **1997**, *163*, 199−215.
(35) Querini, C.; Fung, S. Coke and product profiles formed along the catalyst bed during n-heptane reforming: I. Nonsulfided Pt/Al_2O_3 and $Pt\text{-}Re/Al_2O_3$. *J. Catal.* **1993**, *141*, 389−406.
(36) Izadbakhsh, A.; Khorasheh, F. Simulation of activity loss of fixed bed catalytic reactor of MTO conversion using percolation theory. *Chem. Eng. Sci.* **2011**, *66*, 6199−6208.
(37) Wang, F.; Luo, M.; Xiao, W.; Cheng, X.; Long, Y. Coking behavior of a submicron MFI catalyst during ethanol dehydration to ethylene in a pilot-scale fixed-bed reactor. *Appl. Catal., A* **2011**, *393*, 161−170.
(38) Parera, J.; Beltramini, J.; Querini, C.; Martinelli, E.; Churin, E.; Aloe, P.; Figoli, N. The role of Re and S in the $Pt\text{-}Re\text{-}S\text{-}Al_2O_3$ catalyst. *J. Catal.* **1986**, *99*, 39−52.
(39) Beltramini, J. N.; Wessel, T. J.; Datta, R. Deactivation of the Metal and Acid Functions of Pt/Al_2O_3-Cl Reforming Catalyst by Coke Formation. In *Studies in Surface Science and Catalysis*; Calvin, H. B., John, B. B., Eds.; Elsevier: Amsterdam, 1991; Vol. *68*, pp 119−126.
(40) Zhu, X.; Nie, L.; Lobban, L. L.; Mallinson, R. G.; Resasco, D. E. Efficient conversion of m-cresol to aromatics on a bifunctional Pt/HBeta catalyst. *Energy Fuel* **2014**, *28*, 4104−4111.

DOI: 10.1021/acs.iecr.5b00305
Ind. Eng. Chem. Res. XXXX, XXX, XXX−XXX